MOLECULAR AND CELLULAR BIOLOGY, Jan. 2002, p. 171–181 Vol. 22, No. 1
0270-7306/02/$04.00+0 DOI: 10.1128/MCB.22.1.171–181.2002

Absence of the CAAX Endoprotease Rce1: Effects on Cell Growth and Transformation

Martin O. Bergo,[1,2] Patricia Ambroziak,[1] Cria Gregory,[1] Amanda George,[1] James C. Otto,[3] Edward Kim,[1,2,4] Hiroki Nagase,[5] Patrick J. Casey,[3] Allan Balmain,[5] and Stephen G. Young[1,2,4]*

Gladstone Institute of Cardiovascular Disease, University of California, San Francisco, California 94141-9100[1]; Cardiovascular Research Institute, University of California,[2] and University of California, San Francisco Comprehensive Cancer Center,[5] San Francisco, California 94143; Department of Medicine, University of California, San Francisco, and Medical Service, San Francisco General Hospital, San Francisco, California 94110[4]; and Department of Pharmacology and Cancer Biology, Duke University Medical Center, Durham, North Carolina 27710-3813[3]

Received 19 June 2001/Returned for modification 30 July 2001/Accepted 18 September 2001

After isoprenylation, the Ras proteins and other CAAX proteins undergo two additional enzymatic modifications—endoproteolytic release of the last three amino acids of the protein by the protease Rce1 and methylation of the carboxyl-terminal isoprenylcysteine by the methyltransferase Icmt. This postisoprenylation processing is thought to be important for the association of Ras proteins with membranes. Blocking postisoprenylation processing, by inhibiting Rce1, has been suggested as a potential approach for retarding cell growth and blocking cellular transformation. The objective of this study was to develop a cell culture system for addressing these issues. We generated mice with a conditional *Rce1* allele (*Rce1*^{flox}) and produced *Rce1*$^{flox/flox}$ fibroblasts. *Cre*-mediated excision of *Rce1* (thereby producing *Rce1*$^{\Delta/\Delta}$ fibroblasts) eliminated Ras endoproteolytic processing and methylation and caused a partial mislocalization of truncated K-Ras and H-Ras fusion proteins within cells. *Rce1*$^{\Delta/\Delta}$ fibroblasts grew more slowly than *Rce1*$^{flox/flox}$ fibroblasts. The excision of *Rce1* also reduced Ras-induced transformation, as judged by the growth of colonies in soft agar. The excision of *Rce1* from a *Rce1*$^{flox/flox}$ skin carcinoma cell line also significantly retarded the growth of cells, and this effect was exaggerated by cotreatment of the cells with a farnesyltransferase inhibitor. These studies support the idea that interference with postisoprenylation processing retards cell growth, limits Ras-induced transformation, and sensitizes tumor cells to a farnesyltransferase inhibitor.

After isoprenylation, the Ras proteins as well as other proteins that terminate in a so-called CAAX sequence undergo two sequential enzymatic modifications (38). First, the last three amino acids of the protein (i.e., the AAX of the CAAX sequence) are released by a prenylprotein-specific endoprotease, Rce1 (for Ras-converting enzyme), which is located in the endoplasmic reticulum (ER) (3, 38). Second, the carboxyl group of the newly exposed isoprenylcysteine is methylated (11, 14) by Icmt (for isoprenylcysteine carboxyl methyltransferase). Icmt is also located in the ER (33). These postisoprenylation processing steps are thought to render the carboxyl-terminal domains of CAAX proteins more hydrophobic, facilitating trafficking and the interaction with membranes as well as with protein partners (9, 10, 19, 38).

The CAAX endoprotease Rce1 has attracted attention because it could represent a new target for interfering with the biological activity of CAAX protein substrates. Mutationally activated forms of Ras play a critical role in the development of many human cancers, so the identification of approaches for reducing Ras activity is highly desirable. Recent studies with *Saccharomyces cerevisiae* have suggested that the endoprotease could reduce the activity of mutationally activated Ras proteins (1, 3).

Experimental successes with drugs that block the first step of Ras protein processing, isoprenylation, have already been reported (4, 17, 26, 34). The Ras proteins are isoprenylated by the protein farnesyltransferase, a cytosolic enzyme that transfers a 15-carbon farnesyl group to the cysteine (C) within the carboxyl-terminal CAAX sequence (6). The farnesylation step is critical for Ras activity (23). Protein farnesyltransferase inhibitors interfere with the membrane targeting of Ras proteins and block the growth of tumors and tumor cell lines, particularly those caused by activated forms of H-Ras (26, 29). However, there are questions about whether these agents will be quite as effective against tumors caused by activated forms of K-Ras (the Ras isoform most often implicated in human cancers) because of the existence of an alternate enzymatic pathway for isoprenylation (22). In the setting of farnesyltransferase inhibitors, K-Ras is isoprenylated by another enzyme, protein geranylgeranyltransferase I, which adds a 20-carbon geranylgeranyl group to the protein (22, 38). An attractive feature of Rce1 as a target is that this endoprotease is essential for the processing of all of the Ras proteins, regardless of whether they have been farnesylated or geranylgeranylated (31).

Of note, farnesyltransferase inhibitors are effective against tumors in part by inhibiting the isoprenylation of CAAX proteins aside from the Ras proteins (12, 15, 27, 28). The same

* Corresponding author. Mailing address: Gladstone Institute of Cardiovascular Disease, P.O. Box 419100, San Francisco, CA 94141-9100. Phone: (415) 826-7500. Fax: (415) 285-5632. E-mail: syoung@gladstone.ucsf.edu.

could be the case for inhibitors of the CAAX endoprotease. Thus, it is conceivable that Rce1 inhibition might reduce cell growth and transformation of Ras-transformed cells by affecting the function of non-Ras substrates.

Our laboratory has been interested in evaluating Rce1 as a potential target for modulating the biological activity of prenylated CAAX proteins. Our initial biochemical studies established the essential role of Rce1 in the endoproteolytic processing of mammalian Ras proteins as well as other CAAX proteins (25, 31). Using a conventional gene-targeting vector, we produced *Rce1* knockout mice, with the goal of using those animals to assess the consequences of absent endoproteolytic processing (25). Unfortunately, this goal was largely thwarted by the phenotype of the mice. Homozygous knockout mice ($Rce1^{-/-}$) died during embryonic development, making whole-animal experiments impossible. Fibroblast cell lines could be cultured from $Rce1^{-/-}$ embryos. However, we were reluctant to pursue studies of cell growth and transformation with $Rce1^{-/-}$ and $Rce1^{+/+}$ cell lines—at least as the sole methodological approach—because we were concerned that biological variability in the growth of different embryonic cell lines might make it difficult to identify changes caused by the absence of Rce1, particularly if the changes were modest.

In the present study, we developed a conditional *Rce1* allele and performed gene-excision experiments to define the effect of *Rce1* deficiency on cell growth and on Ras-induced transformation. This approach allowed us to compare phenotypes of normal *Rce1* expression and *Rce1* deficiency in the very same cell line.

MATERIALS AND METHODS

Mice with a conditional *Rce1* allele. A sequence-replacement gene-targeting vector designed to flank *Rce1* with *loxP* sites was constructed in pKS*loxP*NT (21), which contains polylinkers, a thymidine kinase gene (*tk*), and a neomycin resistance gene (*neo*) flanked by *loxP* sites. The vector was constructed with sequences from a 10.5-kb *Bam*HI fragment spanning the *Rce1* gene. The 5′ arm of the vector (a 1.4-kb *Bam*HI-*Eco*RI fragment upstream from the *Rce1* coding sequences) was cloned into the *Bam*HI and *Sal*I sites of pKS*loxP*NT. To generate the 3′ arm, a 4-kb *Eco*RV-*Eco*RI fragment (sequences 3′ to the *Rce1* coding sequences) was inserted into the *Not*I site of pNB1, which contains a polylinker flanked by *loxP* sites. The *Sal*I-*Pvu*II fragment of the resulting plasmid was inserted into the *Xho*I and *Kpn*I sites of pKS*loxP*NT. Finally, a 4-kb *Not*I-*Eco*RV fragment (corresponding to the *Rce1* coding sequences) was inserted into the *Sma*I site of pBlueScript SK (Stratagene, La Jolla, Calif.). The *Bam*HI fragment was removed from that vector and inserted into the *Bam*HI site of pKS*loxP*NT. Thus, the 3′ arm of the vector contained the entire *Rce1* gene (~4 kb) flanked by *loxP* sites and 4 kb of downstream sequences. The vector was electroporated into mouse embryonic stem (ES) cells, and targeted colonies were identified by Southern blot analysis of *Eco*RV-digested genomic DNA with a 1-kb *Bam*HI-*Eco*RI probe located 3′ to the sequences in the gene-targeting vector. Targeted ES cell clones were used to produce mice bearing the conditional *Rce1* allele ($Rce1^{flox}$). As expected, $Rce1^{flox/flox}$ mice were healthy and fertile. The $Rce1^{flox/flox}$ mice had a mixed genetic background (~50% C57BL/6 and ~50% 129/SvJae), were fed a chow diet (Ralston-Purina, St. Louis, Mo.), and were housed in a barrier facility. This work was performed under animal use protocols approved by the University of California, San Francisco.

Generation of fibroblast cell lines from mouse embryos. Primary embryonic fibroblasts were isolated from $Rce1^{flox/flox}$ embryos harvested 13.5 days postcoitum (25, 35). To immortalize the fibroblasts, they were passaged every 3 days for 3 months while maintaining ≥50% confluency. Two separate lines of $Rce1^{flox/flox}$ fibroblasts, A and B, were developed. During spontaneous immortalization, fibroblasts develop mutations, frequently in p53 or p19, that render them susceptible to transformation by activated forms of Ras (39).

We also used primary fibroblasts from *Rce1*-deficient embryos ($Rce1^{-/-}$) and wild-type ($Rce1^{+/+}$) control embryos. Primary fibroblasts cannot be transformed by Ras alone, but can be transformed by the combination of E1A and Ras (24, 39).

Production of $Rce1^{\Delta/\Delta}$ cells with *Cre* adenovirus. To delete *Rce1* from cells (producing $Rce1^{\Delta/\Delta}$ cells), $Rce1^{flox/flox}$ cells were infected with 10^8 PFU of replication-deficient *Cre* adenovirus (AdRSV*Cre*) per ml. Control cells were treated with the same amount of a β-galactosidase adenovirus, AdRSVn*lacZ*. To produce mixed populations of $Rce1^{\Delta/\Delta}$ and $Rce1^{flox/flox}$ cells (i.e., incomplete levels of *Cre*-mediated recombination), $Rce1^{flox/flox}$ cells were infected with AdRSV*Cre* (10^6 or 10^7 PFU/ml) and AdRSVn*lacZ* (10^8 PFU/ml). Identical procedures were used to delete the floxed *neo* gene from $Rce1^{-/-}$ cells.

CAAX endoprotease assay. CAAX endoprotease assays were performed essentially as described previously (25, 31). Human K-Ras, human H-Ras, human N-Ras, bovine $G_{\gamma 1}$, and human Rap1B were expressed in *Escherichia coli* and prenylated in vitro with protein farnesyltransferase or protein geranylgeranyltransferase I. Prenylated protein substrates (final concentration, ~2 μM) and membrane proteins from cells (50 μg) were mixed in 50 μl of a 100 mM HEPES buffer (pH 7.5) containing 5 mM $MgCl_2$. After a 30-min incubation at 37°C, the proteolysis reaction was stopped, and the methyltransferase reaction was initiated by adding a cocktail (20 μl, pH 7.0) containing 5 mM Na_2HPO_4, 87.5 mM EDTA, a variety of protease inhibitors (300 μM *N*-tosyl-L-phenylalanine chloromethylketone, 1 mM phenylmethylsulfonyl fluoride, 10 mM 1,10-phenanthroline), 20 μg of membranes from Sf9 cells expressing yeast Ste14p, and 17.5 μM *S*-adenosyl-L-[*methyl*-^{3}H]methionine (1.5 Ci/mmol). After a 20-min incubation at 37°C, the methylation reaction was terminated by adding 0.5 ml of 4% sodium dodecyl sulfate. Brain cytosol (50 μg protein) was added as a carrier, the mixture was incubated for 20 min at room temperature, and the proteins were precipitated by adding 0.5 ml of 30% trichloroacetic acid. Precipitated proteins were collected on glass fiber filters (the Ras proteins and Rap1B) or nitrocellulose filters ($G_{\gamma 1}$). The extent of endoproteolysis was determined by quantifying ^{3}H incorporation into proteins by scintillation counting. Protease activity was expressed as a percentage of methylation observed when the assay included 0.5 μg of membranes from Sf9 cells overexpressing the human *RCE1* gene.

Subcellular fractionation to assess the localization of Ras proteins in fibroblasts. S100 (cytosolic) and P100 (membrane) fractions of $Rce1^{\Delta/\Delta}$ and $Rce1^{flox/flox}$ cells were isolated according to established methods (13, 25). Ras proteins were immunoprecipitated from the fractions as described in reference 25. Western blots were performed with the Ras-specific monoclonal antibody Ab-4 (Oncogene Science, Uniondale, N.Y.), a horseradish peroxidase-conjugated sheep anti-mouse immunoglobulin G (IgG) (Amersham, Piscataway, N.J.), and the Amersham enhanced chemiluminescence (ECL) kit.

Subcellular localization of Ras proteins with EGFP-truncated Ras fusion proteins. $Rce1^{\Delta/\Delta}$ and $Rce1^{flox/flox}$ fibroblasts were transfected with plasmids coding for fusions between enhanced green fluorescent protein (EGFP) and the carboxyl-terminal tail of the Ras proteins. An EGFP–amino-terminally truncated K-Ras fusion construct, EGFP-tK-Ras (encoding EGFP followed by the carboxyl-terminal 20 amino acids of K-Ras), has been described previously (25). An EGFP–amino-terminally truncated H-Ras fusion (EGFP-tH-Ras) construct, pEGFP-F, was purchased from Clontech (Palo Alto, Calif.). $Rce1^{\Delta/\Delta}$ and $Rce1^{flox/flox}$ fibroblasts were transfected with SuperFect reagent (Qiagen, Valencia, Calif.). Cells were fixed in 4% formalin 24 to 28 h after transfection, mounted, and viewed with a Bio-Rad MRC-600 laser scanning confocal imaging system. The EGFP-tH and EGFP-tK fusion proteins are normally targeted to the inner surface of the plasma membrane, and the purpose of our experiments was to gauge the effect of an *Rce1* excision on this membrane localization.

Assessment of the growth of $Rce1^{\Delta/\Delta}$ and $Rce1^{flox/flox}$ fibroblasts. Small amounts (10^6 or 10^7 PFU) of AdRSV*Cre* were applied to $Rce1^{flox/flox}$ cells to induce moderate levels of recombination, producing mixed cultures of $Rce1^{flox/flox}$ and $Rce1^{\Delta/\Delta}$ cells. The cells were split 1:10 every 3 days. The relative growth rates of $Rce1^{flox/flox}$ and $Rce1^{\Delta/\Delta}$ cells were assessed by using Southern blots to compare the ratios of $Rce1^{flox}$ and $Rce1^{\Delta}$ alleles at different passages. Southern blots were quantified by phosphorimager. In a control experiment, mixed populations of $Rce1^{flox/flox}$ and $Rce1^{\Delta/\Delta}$ cells were grown in the presence of G418 (200 μg/ml). To test the possibility that the excision of *neo* by itself might affect cell growth, AdRSV*Cre* was used to delete a floxed *neo* gene from ~50% of the cells in a culture of $Rce1^{-/-}$ cells (producing a mixed population of $Rce1^{-/-}$ and $Rce1^{-\Delta neo/-\Delta neo}$ cells). The relative growth of $Rce1^{-/-}$ and $Rce1^{-\Delta neo/-\Delta neo}$ cells was assessed by Southern blotting at multiple passages.

$Rce1^{flox/flox}$ and fully deleted $Rce1^{\Delta/\Delta}$ cells were also mixed together and grown for multiple passages, and the ratio of $Rce1^{flox}$ and $Rce1^{\Delta}$ alleles was analyzed at frequent intervals. Some of these "competitive fitness" experiments were performed in the setting of a farnesyltransferase inhibitor, SCH66336, provided by Robert Bishop (Schering-Plough Research Institute, Kenilworth, N.J.).

SCH66336 was prepared in dimethyl sulfoxide; control cells received dimethyl sulfoxide alone.

The relative growth of *Rce1*$^{flox/flox}$ and *Rce1*$^{\Delta/\Delta}$ cells was also compared with an MTS tetrazolium compound-based cell proliferation assay (CellTiter 96 AQueous One Solution cell proliferation assay; Promega, Madison, Wis.). Equal numbers of *Rce1*$^{flox/flox}$ and *Rce1*$^{\Delta/\Delta}$ cells were seeded separately into T25 flasks and allowed to grow for 48 h. Cells from these flasks were counted and seeded into 96-well plates (one plate per time point). In some experiments, SCH66336 was included in the medium. To measure cell growth, 20 μl of MTS reagent added to the cells, which were then incubated at 37°C for 2 h. The reaction was stopped by adding 25 μl of 10% sodium dodecyl sulfate. The amount of formazan produced from the metabolism of the MTS tetrazolium compound was quantified by recording A_{490}.

Assays of anchorage-independent growth. *Rce1*$^{flox/flox}$ cells (60-mm-diameter dishes, 70 to 80% confluent) were infected with retroviruses coding for mutationally activated (Gly12Val) forms of H-Ras or K-Ras (provided by M. McMahon, Cancer Center, University of California, San Francisco). The retroviral stocks were placed on the cells overnight. The next morning, the viral supernatant was replaced with 6 ml of phenol red-free DME supplemented with 20% fetal bovine serum, and the cells were allowed to grow for 72 h. After selection with puromycin (4 μg/ml), Ras overexpression was assessed by Western blotting. Ras-transfected *Rce1*$^{flox/flox}$ fibroblasts were incubated with AdRSVn*lacZ* and AdRSV*Cre* (to produce Ras-transfected *Rce1*$^{\Delta/\Delta}$ cells) or AdRSVn*lacZ* alone (Ras-transfected *Rce1*$^{flox/flox}$ control cells). Equal numbers (3000 cells/well) of Ras-transfected *Rce1*$^{flox/flox}$ or *Rce1*$^{\Delta/\Delta}$ cells were mixed with medium containing 0.35% agarose and poured onto wells of 12-well plates that contained a 0.7% agarose base. The plates were incubated in a humidified culture incubator at 37°C with 7% CO_2 for 14 to 21 days. Colonies were stained with MTT (3-[4,5-dimethylthiazol-2-yl]2,5-diphenyltetrazolium bromide; thiazolyl blue; Sigma) at 1 mg/ml in phosphate-buffered saline. Each well was photographed with a digital camera. The images were imported into Adobe PhotoShop, and colony numbers were determined with an image-processing tool kit, volume 3.0 (http://members.aol.com/ImagProcTK/).

Comparing palmitoylation of H-Ras in *Rce1*$^{flox/flox}$ and *Rce1*$^{\Delta/\Delta}$ cells. To determine if the excision of *Rce1* affected the palmitoylation of the Ras proteins, H-Ras-transfecetd *Rce1*$^{flox/flox}$ and corresponding *Rce1*$^{\Delta/\Delta}$ cells were metabolically labeled with [^{3}H]palmitate, according to the procedures of Mumby and Buss (29a). Fibroblasts were labeled for either 1 or 12 h with palmitate labeling medium (29a) containing supplemental pyruvate and 2.5 mCi of [^{3}H]palmitate (Amersham) per 100-mm dish. Approximately 50% of the label was taken up by the cells at 1 h and 90% was taken up by 12 h. Following the incubation with [^{3}H]palmitate, the Ras proteins were immunoprecipitated with a Ras-specific rat monoclonal antibody as previously described (25). The immunoprecipitate was then size fractionated on a sodium dodecyl sulfate-polyacrylamide gel (10 to 20% gradient) under nonreducing conditions. The proteins were then electrophoretically transferred to a sheet of Hybond-P membrane (Amersham). After the membrane was sprayed with EN^{3}HANCE (New England Nuclear), radiolabeling of the Ras proteins was assessed by autoradiography. In parallel, a separate membrane was prepared to perform Western blot analysis with the Ras-specific mouse monoclonal antibody Ab-4 (25).

Generation and analysis of *Rce1*$^{flox/flox}$ and *Rce1*$^{\Delta/\Delta}$ skin carcinoma cell lines. After the back skin had been shaved, 12 female *Rce1*$^{flox/flox}$ mice were treated weekly with 7,12-dimethylbenz(a)anthracene (DMBA) (25 μg per mouse, in 200 μl of acetone) and 12-*O*-tetradecanoyl-phorbol-13-acetate (TPA) (200 μl of a 5×10^{-5} M solution in acetone) (30). The two treatments were administered 4 days apart, and both were continued for 24 weeks. This protocol results in the formation of papillomas, with a relatively high frequency of conversion to carcinomas by 4 to 6 months. Several skin carcinoma cell lines were prepared, essentially as previously described (18). Briefly, animals were sacrificed, and the skin was soaked in 70% ethanol. Small pieces of skin carcinomas were dissected free from normal tissue, placed in 6-cm-diameter petri dishes, and allowed to adhere to the surface before addition of about 3 ml of Dulbecco's modified Eagle's medium (DMEM) containing 20% fetal bovine serum, hydrocortisone, and antibiotics as previously described (18). After 2 to 4 weeks at 37°C, the explants were removed, and the epithelial cells were trypsinized and expanded. The resulting cultures of epithelial cells were further passaged after ring cloning, and multiple aliquots were frozen in liquid N_2. Cultures with signs of fibroblast contamination were discarded, and only cell lines with cuboidal epithelial morphology were maintained. A single *Rce1*$^{flox/flox}$ skin carcinoma cell line, T22B, was expanded and analyzed. The expression of keratin in that line was documented by Western blotting with an anti-pan-cytokeratin antibody (no. 250400, Calbiochem, La Jolla, Calif.).

Many skin carcinoma cell lines frequently contain a mutationally activated H-Ras caused by a CAA-to-CTA transition at codon 61 (5). To test for this mutation, a 207-bp segment of the H-Ras gene was amplified from the genomic DNA of cell line T22B with oligonucleotides 5′-AAGCCTGTTGTTTTGCAGGA-3′ and 5′-GGTGGCTCACCTGTACTAATG-3′. The Ras mutation can be detected with an *Xba*I digestion (PCR product cleaved into 91- and 116-bp fragments).

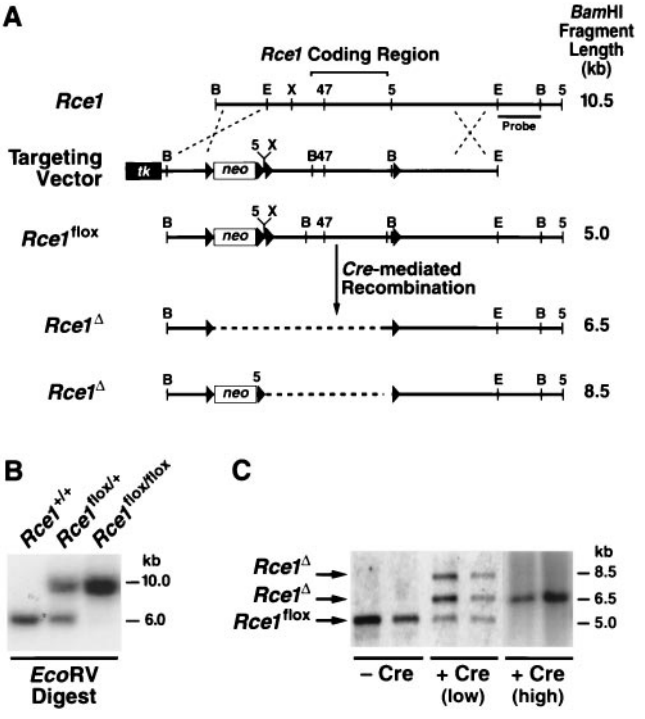

FIG. 1. Production of mice with a conditional *Rce1* allele. (A) Sequence-replacement strategy to introduce *loxP* sites 5′ and 3′ of the *Rce1* protein-coding sequences. Approximately 1 in 200 G418- and FIAU-resistant ES cell clones were targeted and contained all of the *loxP* sites. (B) Southern blot identification of *Rce1*$^{+/+}$, *Rce1*$^{flox/+}$, and *Rce1*$^{flox/flox}$ mice with *Eco*RV-cleaved genomic DNA and a 3′ flanking probe. (C) Southern blot identification of *Cre*-mediated recombination events, with *Bam*HI-cleaved genomic DNA and the same 3′ flanking probe. Shown are examples of *Rce1*$^{flox/flox}$ cells infected with small (10^6 PFU) or large (10^8 PFU) amounts of AdRSV*Cre*.

To produce *Rce1*$^{\Delta/\Delta}$ skin carcinoma cells, *Rce1*$^{flox/flox}$ cells were infected with AdRSV*Cre* (10^8 PFU/ml). The relative growth rates of *Rce1*$^{flox/flox}$ and *Rce1*$^{\Delta/\Delta}$ cells were compared with the MTS tetrazolium compound-based cell proliferation assay described above. In some experiments, cells were incubated with various concentrations of the farnesyltransferase inhibitor SCH66336.

Comparing the ability of Ras-transfected *Rce1*$^{flox/flox}$ and *Rce1*$^{\Delta/\Delta}$ fibroblasts to contribute to the formation of tumors in nude mice. To assess the relative capacities of Ras-transfected *Rce1*$^{flox/flox}$ and *Rce1*$^{\Delta/\Delta}$ fibroblasts to grow in mice, we first generated mixed populations of *Rce1*$^{\Delta/\Delta}$ and *Rce1*$^{flox/flox}$ cells by infecting the *Rce1*$^{flox/flox}$ fibroblasts with AdRSV*Cre* (10^6 PFU/ml) and AdRSVn*lacZ* (10^8 PFU). This mixed population of *Rce1*$^{\Delta/\Delta}$ and *Rce1*$^{flox/flox}$ fibroblasts (2×10^6 viable cells) was injected underneath the skin of NIH Swiss nude mice ($n = 10$) (catalog no. NSWNU-M; Taconic, Germantown, N.Y.). Tumors (mean weight, 1.2 ± 0.22 g) were harvested at 21 days. Genomic DNA from the tumors and from the injected cells was analyzed by Southern blotting and phosphorimager analysis. The relative capacity of *Rce1*$^{flox/flox}$ and *Rce1*$^{\Delta/\Delta}$ cells to contribute to tumors was assessed by quantifying, with Southern blots, the ratio of the *Rce1*^{flox} (5 kb) and *Rce1*$^{\Delta}$ bands (6.5 kb), both in the injected fibroblasts and in the tumors formed from those fibroblasts. In these experiments, we did not have to be concerned about the influence of host DNA, since the *Rce1*$^{+}$ band is 15 kb, and this band did not interfere with the analysis. In control experiments, fibroblasts not transfected with Ras did not produce tumors.

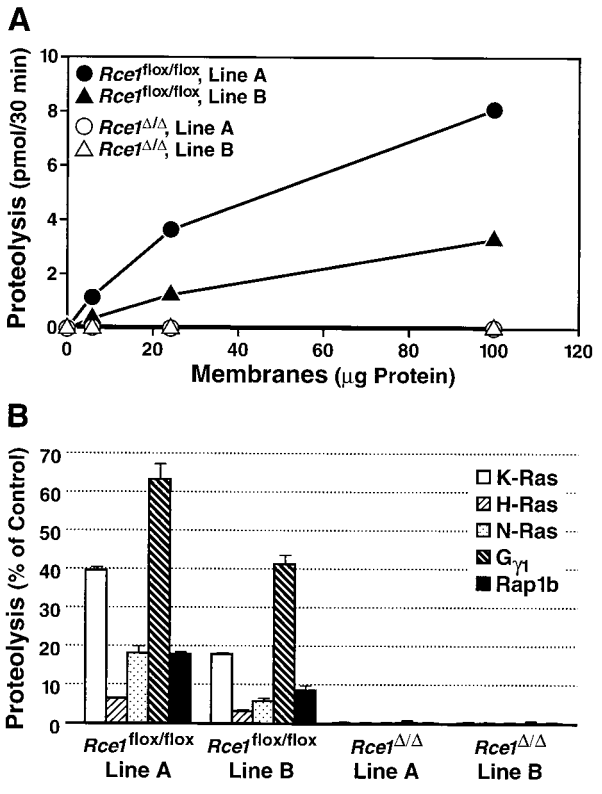

FIG. 2. Rce1 activity in two different immortalized lines (lines A and B) of *Rce1*$^{flox/flox}$ and *Rce1*$^{\Delta/\Delta}$ fibroblasts. (A) Concentration dependence of protease activity in membrane fractions from fibroblasts. Fibroblast membranes (0 to 100 μg) were incubated with 2.0 μM farnesyl–K-Ras for 30 min at 37°C. (B) Endoprotease activity in membranes from *Rce1*$^{flox/flox}$ and *Rce1*$^{\Delta/\Delta}$ fibroblasts against farnesyl–K-Ras, farnesyl–H-Ras, farnesyl–N-Ras, farnesyl-$G_{\gamma 1}$, and geranylgeranyl-Rap1b. Protease activity is expressed as a percentage of the total CAAX protein turnover.

RESULTS

A conditional *Rce1* allele. A conditional *Rce1* allele, *Rce1*^{flox}, was generated by gene-targeting techniques (Fig. 1A and B). To validate the allele, *Rce1*$^{flox/flox}$ embryonic fibroblasts were produced and infected with AdRSV*Cre*. The expected recombination events occurred. When the cells were infected with small amounts of AdRSV*Cre* (10^6 or 10^7 PFU/ml), Southern blots revealed a 6.5-kb *Rce1*$^{\Delta}$ band (reflecting the absence of both *Rce1* and the *neo* gene), an 8.5-kb *Rce1*$^{\Delta}$ band (the absence of *Rce1*, but not the *neo*), and a 5-kb *Rce1*^{flox} band (no recombination) (Fig. 1C). The 8.5-kb *Rce1*$^{\Delta}$ allele represents an incomplete recombination event and was detectable at significant levels only within the first 72 h after AdRSV*Cre* infection. Homogeneous populations of *Rce1*$^{\Delta/\Delta}$ cells (where Southern blots showed the 6.5-kb *Rce1*$^{\Delta}$ band exclusively) were obtained by infecting fibroblasts with larger amounts of AdRSV*Cre* (10^8 PFU/ml) (Fig. 1C).

Absence of CAAX endoprotease activity in *Rce1*$^{\Delta/\Delta}$ fibroblasts. To test the ability of membranes from *Rce1*$^{\Delta/\Delta}$ and *Rce1*$^{flox/flox}$ fibroblasts to process farnesylated K-Ras and other isoprenylated substrates, we used a coupled methylation assay (31). Two different lines of immortalized *Rce1*$^{flox/flox}$ fibroblasts, lines A and B, were generated from different embryos, and *Rce1*$^{\Delta/\Delta}$ fibroblasts were produced from each line. Membrane fractions from both lines of *Rce1*$^{flox/flox}$ fibroblasts processed isoprenylated CAAX proteins in a concentration-dependent fashion; membranes from *Rce1*$^{\Delta/\Delta}$ cells lacked endoprotease activity (Fig. 2).

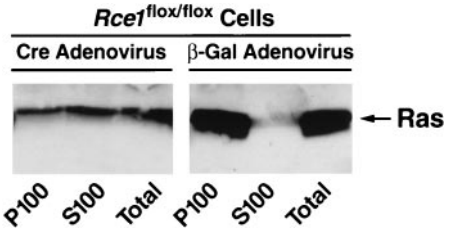

FIG. 3. Intracellular localization of Ras proteins in immortalized fibroblasts. *Cre* adenovirus fully converted *Rce1*$^{flox/flox}$ into *Rce1*$^{\Delta/\Delta}$ fibroblasts. Fibroblasts were fractionated into cytosolic (S100) and membrane (P100) fractions; Ras proteins were immunoprecipitated and analyzed on Western blots of sodium dodecyl sulfate-polyacrylamide gels with antibody Ab-4. Virtually identical results were observed with independently derived lines of *Rce1*$^{flox/flox}$ and *Rce1*$^{\Delta/\Delta}$ fibroblasts (not shown). Also, very similar results were obtained when the experiments were performed with K-Ras-specific antibodies (data not shown).

Ras proteins are mislocalized in *Rce1*$^{\Delta/\Delta}$ fibroblasts. Cell fractionation studies with *Rce1*$^{flox/flox}$ fibroblasts revealed that nearly all of the Ras proteins were in the P100 (membrane) fraction, with very little in the S100 (cytosolic) fraction (Fig. 3). In *Rce1*$^{\Delta/\Delta}$ cells, ~50% of the Ras proteins were in the cytosolic fraction (Fig. 3).

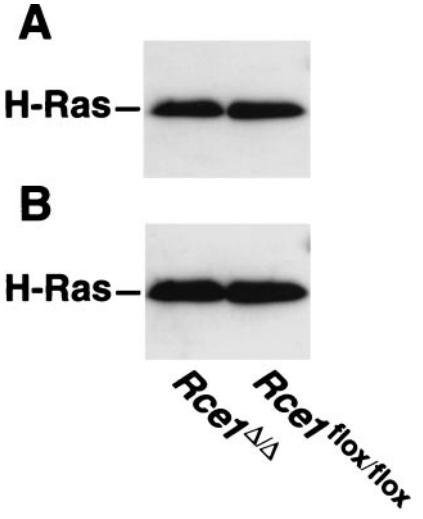

FIG. 4. Palmitoylation of Ras proteins in H-Ras-transfected *Rce1*$^{flox/flox}$ and *Rce1*$^{\Delta/\Delta}$ fibroblasts. (A) Autoradiograph showing the incorporation of [^{3}H]palmitate into immunoprecipitated Ras proteins. Cells were metabolically labeled with [^{3}H]palmitate according to the procedures of Mumby and Buss (29a), and the Ras proteins were immunoprecipitated with a different Ras-specific antibody (25). (B) Western blot of the same immunoprecipitated proteins with a Ras-specific antibody. Note that the Ras proteins from *Rce1*$^{flox/flox}$ and *Rce1*$^{\Delta/\Delta}$ fibroblasts differ very slightly in their electrophoretic mobilities. A slower electrophoretic mobility of Ras proteins in Rce1-deficient cells has been noted previously (25).

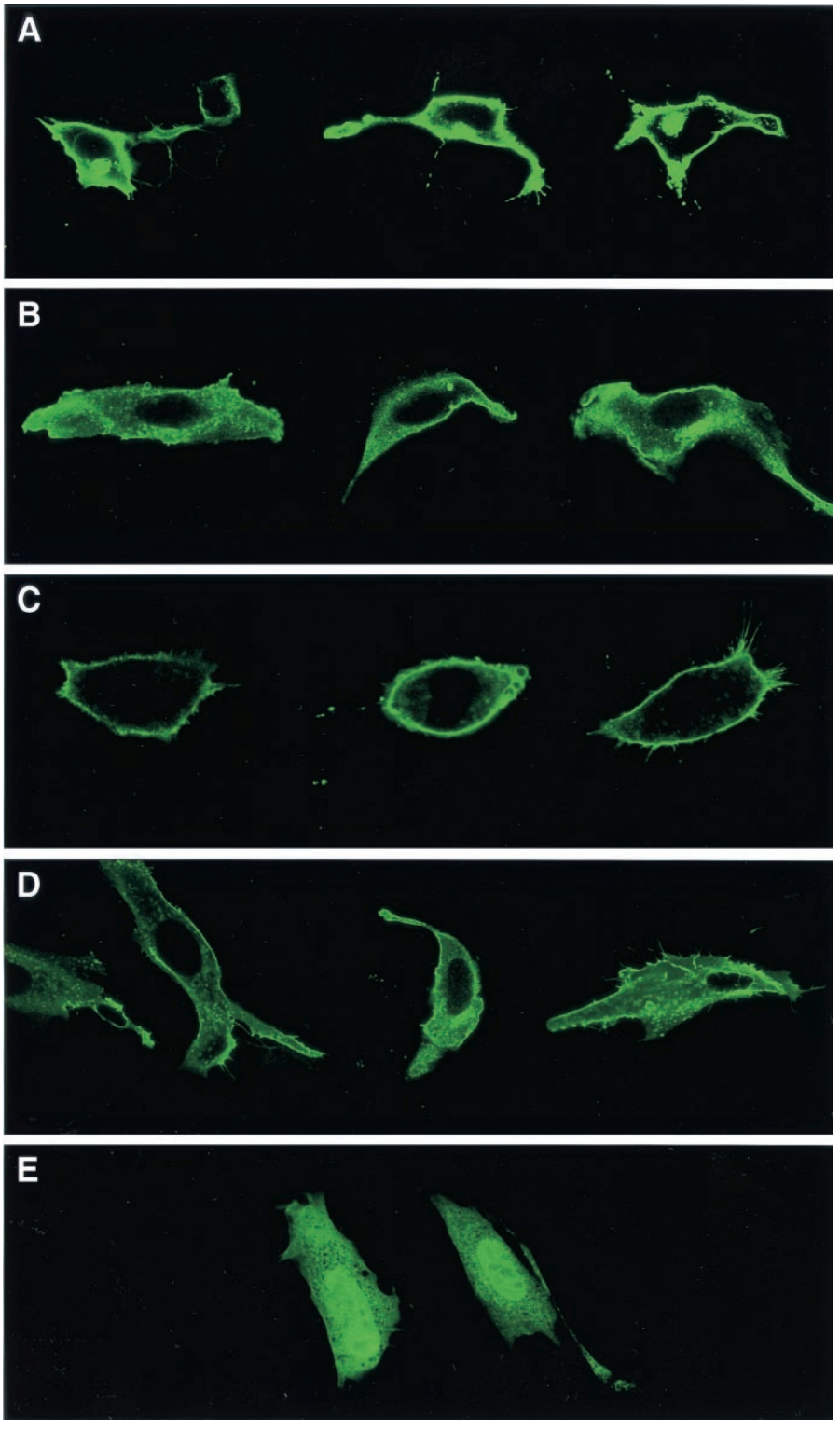

FIG. 5. Confocal microscope images demonstrating the intracellular localization of EGFP-tK-Ras and EGFP-tH-Ras fusions in *Rce1*$^{flox/flox}$ and *Rce1*$^{\Delta/\Delta}$ fibroblasts. Confocal images of *Rce1*$^{flox/flox}$ fibroblasts (A and C) and *Rce1*$^{\Delta/\Delta}$ fibroblasts (B and D) transfected with either EGFP-tH-Ras (A and B) or EGFP-tK-Ras (C and D). (E) Confocal image demonstrating the intracellular localization of an EGFP-tH-Ras fusion in cells treated with a farnesyltransferase inhibitor (SCH66336, 1.0 μM). The genotype of the cell on the left is *Rce1*$^{flox/flox}$; the genotype of the cell on the right is *Rce1*$^{\Delta/\Delta}$. Inhibition of isoprenylation with SCH66336 was associated with the presence of the fusion protein in the nucleus. In viewing many transfected cells under the microscope, we do not believe that the *Rce1* gene excision caused different degrees of mislocalization with the EGFP–tH-Ras and EGFP–tK-Ras fusion proteins.

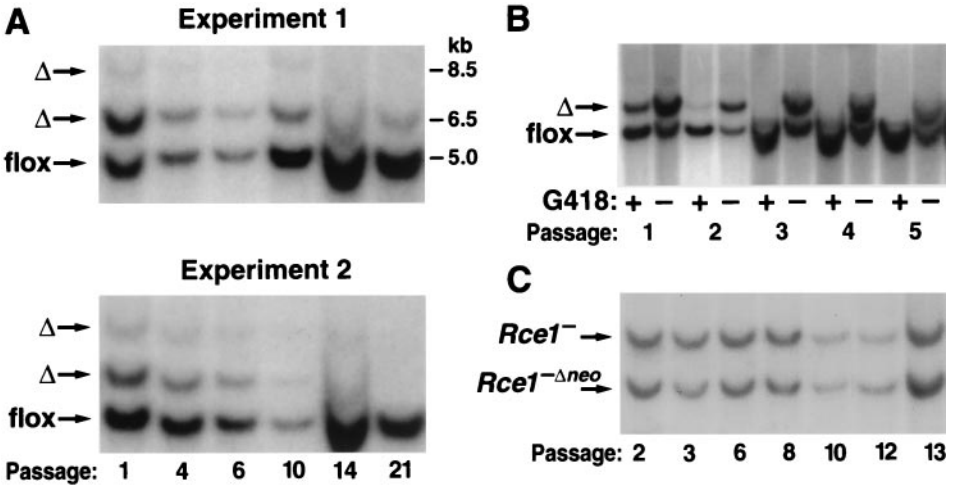

FIG. 6. Southern blot assessment of the ratio of $Rce1^{flox}$ and $Rce1^{\Delta}$ alleles during the growth of mixed cultures of $Rce1^{flox/flox}$ and $Rce1^{\Delta/\Delta}$ fibroblasts. Mixed cultures of $Rce1^{flox/flox}$ and $Rce1^{\Delta/\Delta}$ cells were obtained by infecting immortalized $Rce1^{flox/flox}$ fibroblasts with AdRSVn*lacZ* and AdRSV*Cre* as described in Materials and Methods. (A) Southern blots showing the ratio of $Rce1^{\Delta}$ and $Rce1^{flox}$ alleles at different passages in two independent experiments. Very similar results were obtained with six other experiments involving fibroblasts from two different mouse embryos. (B) Southern blot demonstrating the rapid disappearance of the $Rce1^{\Delta}$ band from a mixed culture of $Rce1^{flox/flox}$ and $Rce1^{\Delta/\Delta}$ cells in the presence of G418. (C) Southern blot showing $Rce1^{-}$ and $Rce1^{-\Delta^{neo}}$ bands during the growth of mixed cultures of $Rce1^{-/-}$ and $Rce1^{-\Delta^{neo}/-\Delta neo}$ cells.

We suspected that the elimination of endoproteolytic processing might indirectly affect the palmitoylation of H-Ras. However, that did not appear to be the case. The amounts of palmitoylation of the Ras proteins in H-Ras-transfected $Rce1^{flox/flox}$ and $Rce1^{\Delta/\Delta}$ cells were virtually identical (Fig. 4).

Ras localization was also assessed by confocal microscopy, following transfection of fibroblasts with EGFP-truncated Ras fusion constructs. The EGFP-tH-Ras fusion was highly localized to the plasma membrane (Fig. 5A), while it was largely cytosolic (or associated with internal membrane compartments) in $Rce1^{\Delta/\Delta}$ cells (Fig. 5B). Similar results were obtained when an EGFP-tK-Ras fusion was transfected into $Rce1^{flox/flox}$ cells (Fig. 5C) and $Rce1^{\Delta/\Delta}$ cells (Fig. 5D). We did observe, with both the tH-Ras and tK-Ras fusions, $Rce1^{\Delta/\Delta}$ cells in which a small amount of the fusion was located along the plasma membrane. This small amount of plasma membrane localization was apparently due to isoprenylation of the protein rather than to nonspecific factors, because it was eliminated when EGFP-tH-Ras-transfected cells were treated with a farnesyltransferase inhibitor (Fig. 5E).

$Rce1^{\Delta/\Delta}$ fibroblasts grow more slowly than $Rce1^{flox/flox}$ fibroblasts. To define the effect of the *Rce1* excision on cell growth, we produced mixed cultures of $Rce1^{flox/flox}$ and $Rce1^{\Delta/\Delta}$ cells by transfecting them with AdRSVn*lacZ* and AdRSV*Cre.* The cells were then allowed to grow for multiple passages, and the *Rce1* genotype was checked by Southern blotting at frequent intervals. If the *Rce1* excision had no effect on cell growth (i.e., if there were no differences in the competitive fitness of $Rce1^{flox/flox}$ and $Rce1^{\Delta/\Delta}$ cells), one would expect that the Southern blots would reveal, over multiple passages, stability in the relative intensities of the 5.0-kb $Rce1^{flox}$ and 6.5-kb $Rce1^{\Delta}$ bands. This was not the case. In each experiment, the ratio of the 5.0-kb $Rce1^{flox}$ to the 6.5-kb $Rce1^{\Delta}$ band increased steadily, indicating a competitive advantage of the $Rce1^{flox/flox}$ cells over $Rce1^{\Delta/\Delta}$ cells (Fig. 6A). In a control experiment, we followed the ratio of the 5.0-kb $Rce1^{flox}$ band to the 6.5-kb $Rce1^{\Delta}$ band when the cells were grown in the presence of G418. Not surprisingly, the $Rce1^{flox}$:$Rce1^{\Delta}$ ratio increased very rapidly, reflecting the fact that $Rce1^{\Delta/\Delta}$ cells lack a *neo* gene and die in the presence of G418 (Fig. 6B).

We considered the possibility that the competitive growth advantage of $Rce1^{flox/flox}$ cells over $Rce1^{\Delta/\Delta}$ cells may have been due simply to the loss of the *neo* (or to the AdRSV*Cre* infection) rather than to the excision of *Rce1*. To examine that possibility, we infected $Rce1^{-/-}$ cells (which contain a floxed *neo* gene) with AdRSV*Cre*, creating a mixed population of $Rce1^{-/-}$ cells and $Rce1^{-\Delta neo/-\Delta neo}$ cells (i.e., $Rce1^{-/-}$ cells in which the *neo* gene is deleted). The $Rce1^{-}$/$Rce1^{-\Delta neo}$ ratio was stable over many passages (Fig. 6C). This finding strongly suggests that the growth advantage of $Rce1^{flox/flox}$ cells over $Rce1^{\Delta/\Delta}$ cells was not simply an artifact caused by the loss of the *neo* gene.

Effects of a farnesyltransferase inhibitor on the growth of $Rce1^{flox/flox}$ and $Rce1^{\Delta/\Delta}$ cells. We hypothesized that the competitive advantage of $Rce1^{flox/flox}$ cells over $Rce1^{\Delta/\Delta}$ cells might be accentuated by a farnesyltransferase inhibitor (SCH66336), which inhibits an earlier step in the same protein modification pathway. To test that hypothesis, we mixed equal numbers of $Rce1^{\Delta/\Delta}$ and $Rce1^{flox/flox}$ cells and grew them in the presence and absence of SCH66336 for multiple passages, periodically checking the intensities of the $Rce1^{\Delta}$ and $Rce1^{flox}$ bands with Southern blots. The farnesyltransferase inhibitor accelerated the disappearance of the $Rce1^{\Delta}$ band (Fig. 7). We also assessed the growth of $Rce1^{\Delta/\Delta}$ and $Rce1^{flox/flox}$ embryonic fibroblasts with a colorimetric cell growth assay and found that the farnesyltransferase inhibitor was particularly potent in slowing the growth of $Rce1^{\Delta/\Delta}$ cells (Fig. 8). The efficacy of SCH66336 in blocking protein farnesylation was documented by demonstrating a reduction in farnesylation (detected as a retarded electrophoretic mobility) of the protein DNAJ (not shown).

Effects of an *Rce1* excision on the growth of Ras-transfected cells in soft agar and in nude mice. In yeast, inactivating *RCE1*

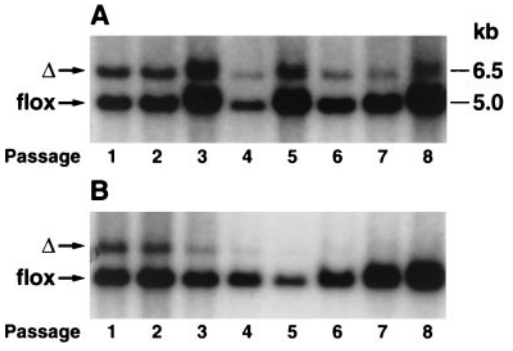

FIG. 7. Southern blot demonstrating the effect of a farnesyltransferase inhibitor on the growth of *Rce1*$^{flox/flox}$ and *Rce1*$^{\Delta/\Delta}$ fibroblasts. *Rce1*$^{flox/flox}$ and *Rce1*$^{\Delta/\Delta}$ fibroblasts in the presence and absence of a farnesyltransferase inhibitor. Approximately equal numbers of *Rce1*$^{flox/flox}$ and *Rce1*$^{\Delta/\Delta}$ fibroblasts were mixed and grown in the absence (A) and presence (B) of a farnesyltransferase inhibitor (SCH66336, 5.0 μM). Southern blots were performed to assess the ratio of *Rce1*^{flox} and *Rce1*$^{\Delta}$ alleles at different passages.

largely blocks the phenotypes associated with a mutationally activated Ras2p (3). In mammalian cells, activated forms of Ras confer upon fibroblasts the ability to grow in soft agar (anchorage-independent growth). To test whether the *Rce1* deletion would influence this phenotype, *Rce1*$^{flox/flox}$ fibroblasts were infected with a retrovirus coding for a mutationally activated K-Ras. We then generated K-Ras-transformed *Rce1*$^{flox/flox}$ and *Rce1*$^{\Delta/\Delta}$ cells and compared their abilities to grow in soft agar. Deletion of *Rce1* resulted in a ~30% reduction in colonies in each of four independent experiments (P = 0.029, P = 0.09, P = 0.005, and P = 0.008), one of which is shown in Fig. 9A. An ~75% reduction in transformed colonies ($P < 0.001$) was observed when a second pair of *Rce1*$^{flox/flox}$ and *Rce1*$^{\Delta/\Delta}$ cells was used (not shown). In parallel experiments, we generated H-Ras-transformed *Rce1*$^{flox/flox}$ and *Rce1*$^{\Delta/\Delta}$ cells and compared their abilities to grow in soft agar. Deletion of *Rce1* resulted in a 65% reduction in colonies (P = 0.002) (Fig. 9B). In multiple experiments, SCH66336 (at concentrations of 1 μM or greater) completely blocked the ability of K-Ras- or H-Ras-transformed cells to form colonies (not shown). Nontransfected immortalized fibroblasts did not form colonies in soft agar.

We also obtained K-Ras-transformed *Rce1*$^{-/-}$ and *Rce1*$^{+/+}$ cells by transfecting primary embryonic fibroblasts with E1A and K-Ras. We then examined *Rce1*$^{-/-}$ and *Rce1*$^{+/+}$ lines that expressed a comparable level of K-Ras (see insert in Fig. 9C) and that had an identical growth rate in culture (not shown). In these experiments, there was an ~50% reduction in numbers of colonies from *Rce1*$^{-/-}$ cells, compared with *Rce1*$^{+/+}$ cells (Fig. 9C). This was the case in three independent experiments (P = 0.003, $P < 0.001$, and $P < 0.001$).

We hypothesized that the reduced ability of K-Ras-transfected *Rce1*$^{\Delta/\Delta}$ cells to grow in soft agar might be associated with reduced capacity to contribute to the growth of tumors in nude mice. To test this hypothesis, we treated K-Ras-transfected *Rce1*$^{flox/flox}$ fibroblasts with AdRSV*Cre,* generating mixed cultures of K-Ras-transfected *Rce1*$^{flox/flox}$ and *Rce1*$^{\Delta/\Delta}$ cells. Those cells were injected into nude mice (n = 10), and tumors were harvested after 21 days. Of note, the *Rce1*$^{flox/flox}$ cells manifested an increased capacity to contribute to the

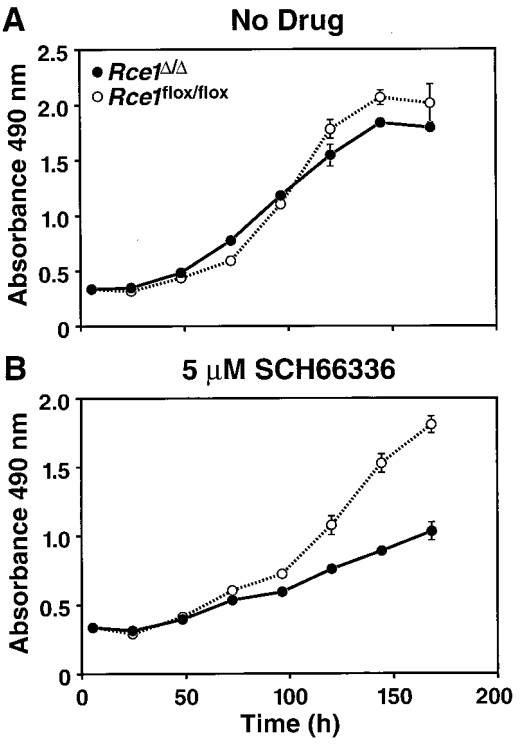

FIG. 8. Growth of *Rce1*$^{\Delta/\Delta}$ and *Rce1*$^{flox/flox}$ fibroblasts in the presence and absence of a farnesyltransferase inhibitor. Equal numbers of *Rce1*$^{flox/flox}$ or *Rce1*$^{\Delta/\Delta}$ fibroblasts were seeded separately onto 96-well plates in medium containing vehicle (dimethyl sulfoxide) alone or vehicle plus different concentrations of SCH66336 (12 wells for each concentration of drug). (A) No SCH66336. (B) SCH66336 at 5 μM. Cell growth was assessed with the CellTiter 96 AQueous One Solution cell proliferation assay (Promega). Gradually increasing differences in the growth rates of *Rce1*$^{flox/flox}$ or *Rce1*$^{\Delta/\Delta}$ fibroblasts were noted with 50 nM SCH66336 and with 1 μM SCH66336 (not shown).

formation of tumors, relative to the *Rce1*$^{\Delta/\Delta}$ cells (Fig. 10). As judged by phosphorimager analysis of Southern blots, the ratio of *Rce1*$^{\Delta}$ to *Rce1*^{flox} alleles in the injected cells was 1.99. The ratio increased to 11.8 ± 2.9 (mean ± standard deviation) in the tumor DNA, reflecting the more rapid growth of *Rce1*$^{flox/flox}$ cells relative to *Rce1*$^{\Delta/\Delta}$ cells.

Production of *Rce1*$^{flox/flox}$ skin carcinoma cells and assessment of the effect of an *Rce1* gene excision on their growth. The studies with fibroblasts showed that the *Rce1* excision retarded cell growth and limited cell transformation. To extend these findings, we produced a *Rce1*$^{flox/flox}$ skin carcinoma cell line, T22B. This skin carcinoma cell line, like many cell lines produced with DMBA and TPA, contained a mutationally activated H-Ras protein. Initially, we treated the *Rce1*$^{flox/flox}$ cells with 10^8 PFU of AdRSV*Cre*. Southern blot analysis revealed that this treatment was effective in deleting *Rce1* from 90% of the cells. Repeatedly, we found that the small fraction of *Rce1*$^{flox/flox}$ cells overgrew the culture within a few days in culture. These experiments strongly suggested that the *Rce1*$^{flox/flox}$ skin carcinoma cells grew more rapidly than the *Rce1*$^{\Delta/\Delta}$ cells.

A complete conversion of *Rce1*$^{flox/flox}$ skin carcinoma cells to *Rce1*$^{\Delta/\Delta}$ cells required that we infect the cells with 10^8 PFU of AdRSV*Cre* in two sequential courses. Immediately after estab-

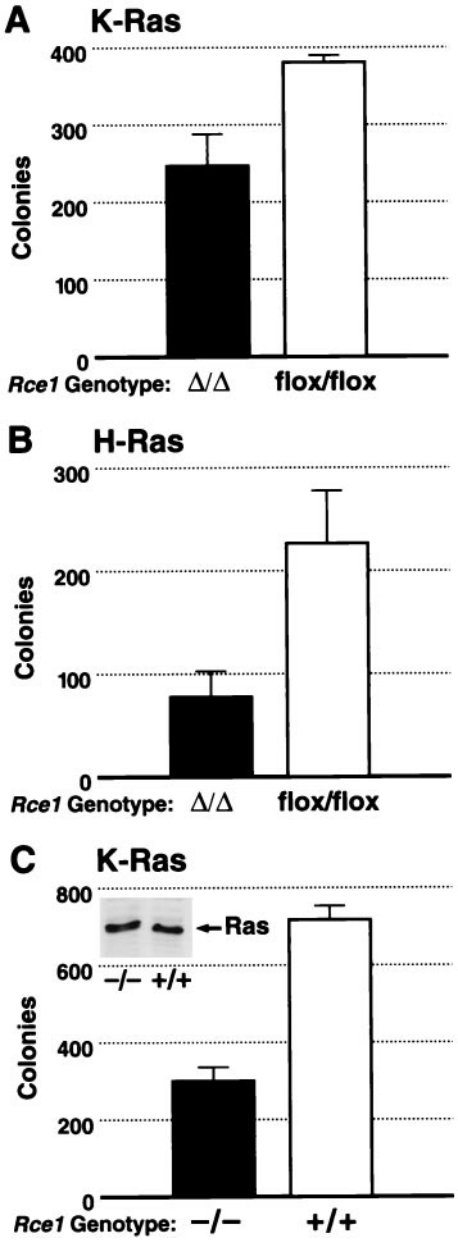

FIG. 9. Comparison of the ability of K-Ras-transformed immortalized *Rce1*$^{\Delta/\Delta}$ and *Rce1*$^{flox/flox}$ fibroblasts to form colonies in soft agar. *Rce1*$^{flox/flox}$ fibroblasts were infected with a K-Ras retrovirus and then treated with either AdRSVn*lacZ* or AdRSV*Cre*. (A) The ability of K-Ras-transformed *Rce1*$^{\Delta/\Delta}$ and *Rce1*$^{flox/flox}$ fibroblasts to grow in soft agar ($P = 0.029$). Similar results were observed in three other independent experiments ($P = 0.005$, $P = 0.09$, and $P = 0.008$). (B) The ability of H-Ras-transformed *Rce1*$^{\Delta/\Delta}$ and *Rce1*$^{flox/flox}$ fibroblasts to grow in soft agar ($P = 0.002$). (C) Comparison of the ability of primary *Rce1*$^{-/-}$ and *Rce1*$^{+/+}$ fibroblasts, matched for K-Ras expression (note Western blot insert), to form colonies in soft agar after transformation with E1A and K-Ras ($P = 0.003$). Similar results were observed in two other experiments ($P < 0.001$ and $P < 0.001$).

lishment of pure cultures of *Rce1*$^{flox/flox}$ and *Rce1*$^{\Delta/\Delta}$ skin carcinoma cells, growth rates were compared with the MTS tetrazolium compound-based cell proliferation assay, in both the presence and absence of the farnesyltransferase inhibitor

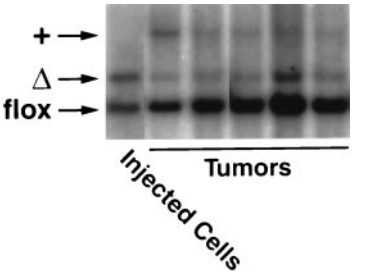

FIG. 10. Southern blot demonstrating the relative ability of mixed cultures of K-Ras-transfected *Rce1*$^{flox/flox}$ and *Rce1*$^{\Delta/\Delta}$ fibroblasts to form tumors in nude mice. Mixed cultures of the fibroblasts were obtained by infecting K-Ras-transfected *Rce1*$^{flox/flox}$ fibroblasts with AdRSVn*lacZ* and AdRSV*Cre* as described in Materials and Methods. Cells were grown for several passages, and then a total of 2×10^6 cells were injected into nude mice ($n = 10$). A Southern blot showed the ratio of *Rce1*$^{\Delta}$ and *Rce1*^{flox} alleles in the injected cells and in the tumors generated from the cells. As judged by a phosphorimager, the *Rce1*^{flox}/*Rce1*$^{\Delta}$ ratio in the injected cells was 1.99; in the tumors, the ratio was 11.8 ± 2.9 (mean $\pm$ SD).

SCH66336. In the absence of the drug, *Rce1*$^{\Delta/\Delta}$ cells grew about one-half as fast as the parental *Rce1*$^{flox/flox}$ cells (Fig. 11A). The difference in growth rate was exaggerated by increasing concentrations of SCH66336 (Fig. 11B to D). At the highest concentration (5 μM), the *Rce1*$^{flox/flox}$ cells continued to grow, but the growth of *Rce1*$^{\Delta/\Delta}$ cells was almost completely inhibited (Fig. 11D).

DISCUSSION

Studies with *S. cerevisiae* demonstrated that the inactivation of Rce1p has little effect on the growth of cells under standard conditions, but largely blocks phenotypes associated with the expression of a mutationally activated form of Ras2p, such as increased sensitivity to heat shock (3). In mammalian cells, activated forms of Ras can turn on signaling pathways that stimulate cell growth and division and can also transform cells, allowing them to grow in an anchorage-independent fashion. In the present study, we sought to develop a cell culture system for defining the consequences of *Rce1* deficiency on cell growth and transformation.

Our basic approach was to generate *Rce1*$^{flox/flox}$ cells and corresponding lines of *Rce1*$^{\Delta/\Delta}$ cells and to compare their properties. As expected, the excision of *Rce1* abolished CAAX endoprotease activity. It also resulted in a rather striking mislocalization of both EGFP–tH-Ras and EGFP–tK-Ras fusions within cells. In immortalized fibroblasts, the excision of the *Rce1* gene clearly retarded the growth of cells in culture. The *Rce1* inactivation also compromised the ability of Ras-transfected *Rce1*$^{\Delta/\Delta}$ fibroblasts to grow in nude mice, relative to the parental *Rce1*$^{flox/flox}$ fibroblasts. The effects of the *Rce1* gene excision on cell growth were even more striking in skin carcinoma cells. The *Rce1* excision also reduced the capacity of Ras-transfected immortalized fibroblasts to form colonies in soft agar—a standard measure of cell transformation.

While the effects of the *Rce1* excision on the anchorage-independent growth of Ras-transfected fibroblasts were unequivocal and reproducible, they were not as quantitatively dramatic as the effects of the farnesyltransferase inhibitor, which abolished colony formation. One could reasonably pos-

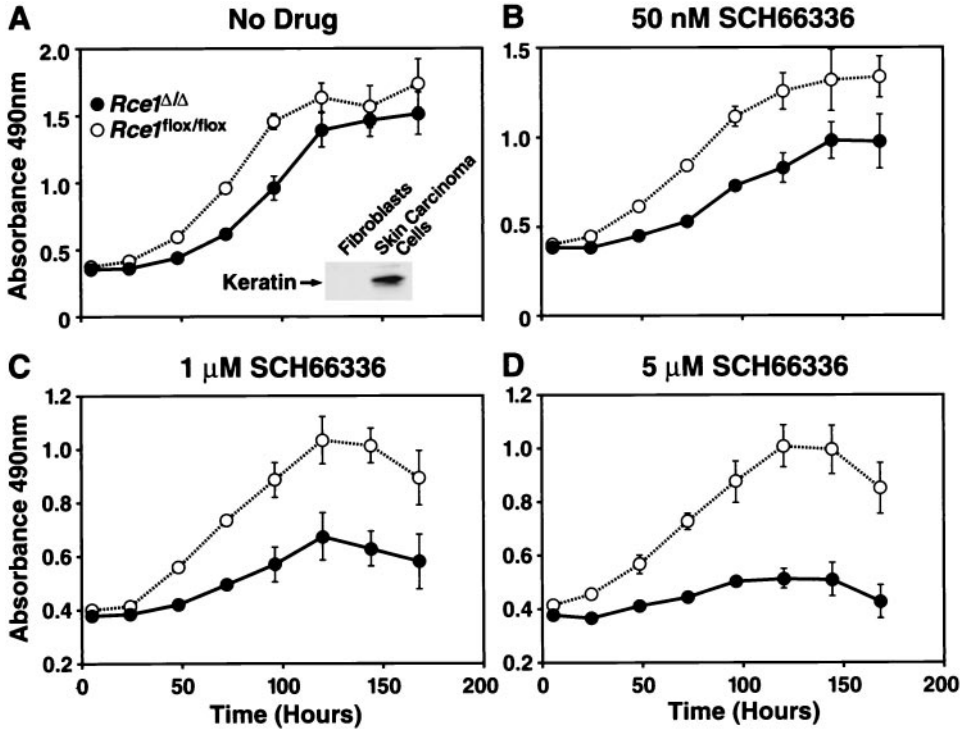

FIG. 11. Growth of *Rce1*$^{\Delta/\Delta}$ and *Rce1*$^{flox/flox}$ skin carcinoma cells in the presence and absence of a farnesyltransferase inhibitor. Equal numbers of *Rce1*$^{flox/flox}$ skin carcinoma cells (cells treated with AdRSVn*lacZ*) and *Rce1*$^{\Delta/\Delta}$ cells (treated with AdRSVn*lacZ* and AdRSV*Cre*) were seeded separately onto 96-well plates in medium containing vehicle (dimethyl sulfoxide) alone or vehicle plus different concentrations of SCH66336 (12 wells for each concentration of drug). (A) No SCH66336. The insert shows a Western blot documenting the expression of keratin in the skin carcinoma cells. (B) SCH66336 at 50 nM. (C) SCH66336 at 1 μM. (D) SCH66336 at 5 μM. Cell growth was assessed with the CellTiter 96 AQueous One Solution cell proliferation assay (Promega). This experiment was representative of three separate experiments.

tulate that the rather striking mislocalization of the Ras proteins (and perhaps other CAAX proteins as well) in the setting of *Rce1* deficiency was simply not sufficient to completely eliminate colony formation. As judged by confocal microscopy, the *Rce1* excision reduced the amount of EGFP-truncated Ras fusion proteins at the plasma membrane significantly, but some still appeared along the plasma membrane. Without question, the mislocalization of the EGFP-tH-Ras fusion protein was more complete in the setting of the farnesyltransferase inhibitor. It is quite possible that a full blockade of the biological effects of an activated Ras requires this more complete mislocalization.

Our studies of the effect of *Rec1* on Ras localization are subject to several caveats. In interpreting experiments with EGFP–t-Ras fusions, it is important to be aware of the fact that these fusions do not necessarily bind to the same specific plasma membrane sites as full-length Ras proteins. Prior and coworkers (32) have found that full-length Ras proteins and GFP-truncated Ras fusions bind to different sites along the plasma membrane (bulk plasma membrane versus lipid rafts and caveolae); this was particularly evident in the case of H-Ras. The same authors have shown that the binding of H-Ras to different locations in the plasma membrane is dynamic, changing depending on GTP binding (32). Our studies do not define what effect, if any, endoproteolysis has on binding of the Ras proteins to lipid rafts. If endoproteolysis were to affect the binding of Ras proteins to specific domains of the plasma membrane, one could easily imagine that this could have functional consequences.

The effects of *Rce1* deficiency are reminiscent of the phenotype associated with K-Ras mutants lacking the polybasic domain near the carboxyl terminus of that protein (20, 36). Hancock and coworkers (20) found that the deletion of the K-Ras polybasic domain (which does not interfere with farnesylation) results in mislocalization of the protein within cells, but produced only a mild to moderate decrease in transforming activity (20). However, we would caution against viewing the *Rce1* gene excision as being equivalent to mutating the carboxyl terminus of a Ras protein. Rce1 has many substrates aside from the Ras proteins, and it is quite possible that the growth and transformation phenotypes that we observed with *Rce1* deficiency could relate, either partly or largely, to blocking the processing of other non-Ras CAAX proteins. Notably, several lines of evidence have suggested that farnesyltransferase inhibitors inhibit Ras-induced cellular transformation by blocking the processing of other CAAX proteins (15, 16, 27, 28).

The results of our studies are in line with results of an inhibitor study by Chen (8). In that study, two inhibitors of CAAX endoprotease activity, *N*-tert-butyloxycarbonyl-(*S*-farnesyl-C)-chloromethyl ketone and *N*-tert-butyloxycarbonyl-2 amino-DL-hexadecanoyl-chloromethyl ketone, were found to inhibit the growth of several mammalian cell lines. The compounds had no effect on the growth of nontransformed mouse 3T3 fibroblasts, but inhibited the growth of K-Ras-transformed

mouse embryonic fibroblasts by ~30%. Low concentrations of the compounds almost completely abolished the ability of K-Ras-transformed rat kidney cells to grow in an anchorage-independent fashion. These results by Chen (8) should, however, be interpreted with some caution, since there was no demonstration that the drugs actually entered the cells or that they inhibited Rce1.

The finding that the farnesyltransferase inhibitor was more potent in inhibiting cell growth in *Rce1*$^{\Delta/\Delta}$ fibroblasts and skin carcinoma cells was intriguing. One way of thinking about this is that the *Rce1* excision has a significant impact on the function of the subset of CAAX proteins that escaped the pharmacological inhibition and thus were farnesylated normally. Another interpretation takes into account the fact that many CAAX proteins, including K-Ras and N-Ras, are geranylgeranylated in the setting of farnesyltransferase inhibition (37). Thus, it is possible that the observed synergism between farnesyltransferase inhibitors and *Rce1* deficiency might be due to the fact that Rce1 inhibition adversely affects the function of those alternately prenylated substrates. Whatever the mechanism, our experiments suggest the possibility that combined inhibition of the isoprenylation and endoprotease steps would be synergistic in retarding the growth of tumor cells.

The conditional gene excision approach allowed us to be confident regarding the phenotypic consequences of *Rce1* deficiency. Most of our cell growth and transformation assays involved direct comparisons of *Rce1*$^{flox/flox}$ cells and the *Rce1*$^{\Delta/\Delta}$ cells derived from them, making it possible to assess the consequences of a single genetic difference (i.e., the knockout mutation). These direct *Rce1*$^{flox/flox}$-*Rce1*$^{\Delta/\Delta}$ comparisons were very sensitive and allowed us to define, quite unequivocally, distinct properties for *Rce1*-deficient cells. Had we adopted the approach of comparing multiple lines of *Rce1*$^{+/+}$ and *Rce1*$^{-/-}$ embryonic fibroblasts (from the conventional knockout experiments), uncovering these differences could have posed a challenge, since we would have had to worry about genetic differences between different outbred embryos as well as differences arising from independent immortalization events. We suspect that the gene excision strategy that we used in these studies will be very useful for analyzing other enzymes involved in the posttranslational modification of CAAX proteins, such as farnesyltransferase (6, 7) and isoprenylcysteine carboxyl methyltransferase (2, 14).

ACKNOWLEDGMENTS

This work was supported in part by NIH grants HL41633 and AG15451 to S.G.Y. and GM46372 to P.J.C, as well as grants from the University of California Tobacco-related Disease Research Program to M.O.B. and S.G.Y. and the Swedish Cancer Foundation to M.O.B.

We thank M. McMahon of the UCSF Cancer Center for helpful advice and for the H-Ras and K-Ras retroviruses, R. Bishop (Schering-Plough, Kenilworth, N.J.) for the farnesyltransferase inhibitor, J. Buss for advice on palmitate labeling of proteins, F. Graham for the *Cre* adenovirus, D. Dichek for assistance with the preparation of adenoviruses, and Reyno Delrosario and Xiaoli Zhang for assistance with carcinoma induction and cell culture studies. We thank Gary Howard and Stephen Ordway for comments on the manuscript.

M.O.B. and P.A. are co-first authors.

REFERENCES

1. **Ashby, M. N., and J. Rine.** 1995. Ras and **a**-factor converting enzyme. Methods Enzymol. **250:**235–251.
2. **Bergo, M. O., G. K. Leung, P. Ambroziak, J. C. Otto, P. J. Casey, and S. G. Young.** 2000. Targeted inactivation of the isoprenylcysteine carboxyl methyltransferase gene causes mislocalization of K-Ras in mammalian cells. J. Biol. Chem. **275:**17605–17610.
3. **Boyartchuk, V. L., M. N. Ashby, and J. Rine.** 1997. Modulation of Ras and a-factor function by carboxyl-terminal proteolysis. Science **275:**1796–1800.
4. **Brown, M. S., and J. L. Goldstein.** 1993. Protein prenylation. Mad bet for Rab. Nature **366:**14–15.
5. **Chakravarti, D., P. Mailander, J. Franzen, S. Higginbotham, E. L. Cavalieri, and E. G. Rogan.** 1998. Detection of dibenzol*[a,l]*pyrene-induced H-*ras* codon 61 mutant genes in preneoplastic SENCAR mouse skin using a new PCR-RFLP method. Oncogene **16:**3203–3210.
6. **Chen, W.-J., D. A. Andres, J. L. Goldstein, D. W. Russell, and M. S. Brown.** 1991. cDNA cloning and expression of the peptide-binding β subunit of rat p21^{ras} farnesyltransferase, the counterpart of yeast DPR1/RAM1. Cell **66:** 327–334.
7. **Chen, W.-J., J. F. Moomaw, L. Overton, T. A. Kost, and P. J. Casey.** 1993. High level expression of mammalian protein farnesyltransferase in a baculovirus system. The purified protein contains zinc. J. Biol. Chem. **268:**9675–9680.
8. **Chen, Y.** 1998. Inhibition of K-*ras*-transformed rodent and human cancer cell growth via induction of apoptosis by irreversible inhibitors of Ras endoprotease. Cancer Lett. **131:**191–200.
9. **Chen, Z., J. C. Otto, M. O. Bergo, S. G. Young, and P. J. Casey.** 2000. The C-terminal polylysine region and methylation of K-Ras are critical for the interaction between K-Ras and microtubules. J. Biol. Chem. **275:**41251–41257.
10. **Choy, E., V. K. Chiu, J. Silletti, M. Feoktistov, T. Morimoto, D. Michaelson, I. E. Ivanov, and M. R. Philips.** 1999. Endomembrane trafficking of Ras: the CAAX motif targets proteins to the ER and Golgi. Cell **98:**69–80.
11. **Clarke, S., J. P. Vogel, R. J. Deschenes, and J. Stock.** 1988. Posttranslational modification of the Ha-*ras* oncogene protein: evidence for a third class of protein carboxyl methyltransferases. Proc. Natl. Acad. Sci. USA **85:**4643–4647.
12. **Cox, A. D., and C. J. Der.** 1997. Farnesyltransferase inhibitors and cancer treatment: targeting simply Ras? Biochim. Biophys. Acta **1333:**F51–F71.
13. **Cox, A. D., P. A. Solski, J. D. Jordan, and C. J. Der.** 1995. Analysis of Ras protein expression in mammalian cells. Methods Enzymol. **255:**195–220.
14. **Dai, Q., E. Choy, V. Chiu, J. Romano, S. R. Slivka, S. A. Steitz, S. Michaelis, and M. R. Philips.** 1998. Mammalian prenylcysteine carboxyl methyltransferase is in the endoplasmic reticulum. J. Biol. Chem. **273:**15030–15034.
15. **Du, W., P. F. Lebowitz, and G. C. Prendergast.** 1999. Cell growth inhibition by farnesyltransferase inhibitors is mediated by gain of geranylgeranylated RhoB. Mol. Cell. Biol. **19:**1831–1840.
16. **Du, W., P. F. Lebowitz, and G. C. Prendergast.** 1999. Elevation of α2(I) collagen, a suppressor of Ras transformation, is required for stable phenotypic reversion by farnesyltransferase inhibitors. Cancer Res. **59:**2059–2063.
17. **Gibbs, J. B., A. Oliff, and N. E. Kohl.** 1994. Farnesyltransferase inhibitors: Ras research yields a potential cancer therapeutic. Cell **77:**175–178.
18. **Haddow, S., D. J. Fowlis, K. Parkinson, R. J. Akhurst, and A. Balmain.** 1991. Loss of growth control by TGF-beta occurs at a late stage of mouse skin carcinogenesis and is independent of Ras gene activation. Oncogene **6:**1465–1470.
19. **Hancock, J. F., K. Cadwallader, and C. J. Marshall.** 1991. Methylation and proteolysis are essential for efficient membrane binding of prenylated p21$^{K\text{-}ras(B)}$. EMBO J. **10:**641–646.
20. **Hancock, J. F., H. Paterson, and C. J. Marshall.** 1990. A polybasic domain or palmitoylation is required in addition to the CAAX motif to localize p21^{ras} to the plasma membrane. Cell **63:**133–139.
21. **Hanks, M., W. Wurst, L. Anson-Cartwright, A. B. Auerbach, and A. L. Joyner.** 1995. Rescue of the *En-1* mutant phenotype by replacement of *En-1* with *En-2*. Science **269:**679–682.
22. **James, G., J. L. Goldstein, and M. S. Brown.** 1996. Resistance of K-RasB^{V12} proteins to farnesyltransferase inhibitors in Rat1 cells. Proc. Natl. Acad. Sci. USA **93:**4454–4458.
23. **Kato, K., A. D. Cox, M. M. Hisaka, S. M. Graham, J. E. Buss, and C. J. Der.** 1992. Isoprenoid addition to Ras protein is the critical modification for its membrane association and transforming activity. Proc. Natl. Acad. Sci. USA **89:**6403–6407.
24. **Kelekar, A., and M. D. Cole.** 1986. Tumorigenicity of fibroblast lines expressing the adenovirus E1a, cellular p53, or normal c-*myc* genes. Mol. Cell. Biol. **6:**7–14.
25. **Kim, E., P. Ambroziak, J. C. Otto, B. Taylor, M. Ashby, K. Shannon, P. J. Casey, and S. G. Young.** 1999. Disruption of the mouse *Rce1* gene results in defective Ras processing and mislocalization of Ras within cells. J. Biol. Chem. **274:**8383–8390.
26. **Kohl, N. E., F. R. Wilson, S. D. Mosser, E. Giuliani, S. J. DeSolms, M. W. Conner, N. J. Anthony, W. J. Holtz, R. P. Gomez, T.-J. Lee, R. L. Smith, S. L. Graham, G. D. Hartman, J. B. Gibbs, and A. Oliff.** 1994. Protein farnesyltransferase inhibitors block the growth of *ras*-dependent tumors in nude mice. Proc. Natl. Acad. Sci. USA **91:**9141–9145.
27. **Lebowitz, P. F., and G. C. Prendergast.** 1998. Non-Ras targets of farnesyltransferase inhibitors: focus on Rho. Oncogene **17:**1439–1445.
28. **Liu, A.-X., W. Du, J.-P. Liu, T. M. Jessell, and G. C. Prendergast.** 2000.

RhoB alteration is necessary for apoptotic and antineoplastic responses to farnesyltransferase inhibitors. Mol. Cell. Biol. **20:**6105–6113.
29. **Liu, M., M. S. Bryant, J. Chen, S. Lee, B. Yaremko, Z. Li, J. Dell, P. Lipari, M. Malkowski, N. Prioli, R. R. Rossman, W. A. Korfmacher, A. A. Nomeir, C.-C. Lin, A. K. Mallams, R. J. Doll, J. J. Catino, V. M. Girijavallabhan, P. Kirschmeier, and W. R. Bishop.** 1999. Effects of SCH 59228, an orally bioavailable farnesyl protein transferase inhibitor, on the growth of oncogene-transformed fibroblasts and a human colon carcinoma xenograft in nude mice. Cancer Chemother. Pharmacol. **43:**50–58.
29a. **Mumby, S. M., and J. M. Buss.** 1990. Metabolic radiolabeling techniques for identification of prenylated and fatty acylated proteins. Methods **1:**216–220.
30. **Naito, M., K. J. Chenicek, Y. Naito, and J. DiGiovanni.** 1988. Susceptibility to phorbol ester skin tumor promotion in (C57BL/6 X DBA/2) mice is inherited as an incomplete dominant trait: evidence for multi-locus involvement. Carcinogenesis **9:**639–645.
31. **Otto, J. C., E. Kim, S. G. Young, and P. J. Casey.** 1999. Cloning and characterization of a mammalian prenyl protein-specific protease. J. Biol. Chem. **274:**8379–8382.
32. **Prior, I. A., A. Harding, J. Yan, J. Sluimer, R. G. Parton, and J. F. Hancock.** 2001. GTP-dependent segregation of H-ras from lipid rafts is required for biological activity. Nat. Cell. Biol. **3:**368–375.
33. **Schmidt, W. K., A. Tam, K. Fujimura-Kamada, and S. Michaelis.** 1998. Endoplasmic reticulum membrane localization of Rce1p and Ste24p, yeast proteases involved in carboxyl-terminal CAAX protein processing and amino-terminal a-factor cleavage. Proc. Natl. Acad. Sci. USA **95:**11175–11180.
34. **Tamanoi, F.** 1993. Inhibitors of Ras farnesyltransferases. Trends Biochem. Sci. **18:**349–353.
35. **Todaro, G. J., and H. Green.** 1963. Quantitative studies of the growth of mouse embryo cells in culture and their development into established lines. J. Cell Biol. **17:**299–313.
36. **Welman, A., M. M. Burger, and J. Hagmann.** 2000. Structure and function of the C-terminal hypervariable region of K-Ras4B in plasma membrane targetting and transformation. Oncogene **19:**4582–4591.
37. **Whyte, D. B., P. Kirschmeier, T. N. Hockenberry, I. Nunez-Oliva, L. James, J. J. Catino, W. R. Bishop, and J.-K. Pai.** 1997. K- and N-Ras are geranylgeranylated in cells treated with farnesyl protein transferase inhibitors. J. Biol. Chem. **272:**14459–14464.
38. **Young, S. G., P. Ambroziak, E. Kim, and S. Clarke.** 2000. Postisoprenylation protein processing: CXXX (CaaX) endoproteases and isoprenylcysteine carboxyl methyltransferase, p. 155–213. *In* F. Tamanoi and D. S. Sigman (ed.), The enzymes. Academic Press, San Diego, Calif.
39. **Zindy, F., C. M. Eischen, D. H. Randle, T. Kamijo, J. L. Cleveland, C. J. Sherr, and M. F. Roussel.** 1998. Myc signaling via the ARF tumor suppressor regulates p53-dependent apoptosis and immortalization. Genes Dev. **12:**2424–2433.